



# Only frequency domain diffractive deep neural networks

**MINGZHU SONG,<sup>1,2</sup> RUNZE LI,<sup>1,2</sup> AND JUNSHENG WANG<sup>1,2,\*</sup>** <sup>1</sup>*Liaoning Key Laboratory of Marine Sensing and Intelligent Detection, Dalian Maritime University, Dalian 116026, China*<sup>2</sup>*Department of Information Science and Technology, Dalian Maritime University, Dalian 116026, China**\*Corresponding author: wangjsh@dlmu.edu.cn**Received 14 November 2022; revised 27 December 2022; accepted 29 December 2022; posted 9 January 2023; published 30 January 2023*

Diffractive deep neural networks (D2NNs) have demonstrated their importance in performing various all-optical machine learning tasks such as classification and segmentation. However, current D2NNs can only detect spatial domain intensity information. They cannot solve problems that rely on frequency information, such as laser linewidth compression. We propose a new D2NN architecture that fully exploits frequency domain information. We demonstrate that only frequency domain D2NN (OF-D3NN) can be trained using deep learning algorithms and be successfully integrated into a free-space optical communications system (FSO) for information recovery. © 2023 Optica Publishing Group

<https://doi.org/10.1364/AO.480640>

## 1. INTRODUCTION

Relying on the development of integrated circuits and the continuous improvement of computer computing power, deep neural networks have solved many cutting-edge problems in the field of artificial intelligence [1,2]. However, the large-scale deployment of traditional neural networks structures that rely on electrons and transistors based on the von Neumann system consumes a lot of resources and energy, resulting in a significant burden. With the gradual failure of Moore's law, the development of neural networks has entered a bottleneck [3]. Finding new network structures has become a hot issue for researchers [4,5]. Photons have the characteristics of anti-electromagnetic interference, speed of light propagation, arbitrary superposition, and low power consumption, which can overcome the fundamental limitations of electrons. This makes calculations that rely on optics much more efficient than relying on electrons. Therefore, optical neural networks, which is an alternative to electronic neural networks, has become a hot topic in the current artificial intelligence community [6].

The field is developing rapidly, and the research on D2NN has shown that, compared to an electronic neural network (ENN), the reasoning capabilities of D2NN can effectively solve most complex computing problems, such as logical operations, target recognition and detection, and beam steering [7–11]. However, in general, most of the parameters obtained in previous studies on diffraction networks are purely theoretical calculations based on computers, and the various errors are rarely considered. Therefore, the networks are susceptible to real-world optical conditions. The optical conditions we can expect mainly fall into three categories: the frequency shift of the light wave caused by the optical Doppler effect; the inherent

linewidth problem and frequency noise of the laser; and the wavefront phase distortion caused by atmospheric turbulence. These effects limit its ability to handle more advanced computer tasks and integration with other optics. More importantly, it is difficult for existing diffraction networks trained based on spatial light intensity to optimize such problems with indistinct spatial features [4]. Although some scholars have studied D2NN based on the frequency domain before, they have not completely separated from the spatial domain. For example, a loss function optimized based on spatial light intensity information is still used, so the problems mentioned above still exist [7,12,13].

Therefore, to alleviate the impact of these problems on the network performance, we propose a diffraction network, OF-D3NN, which is completely based on the frequency domain and is robust to frequency errors. Unlike previous diffraction networks, OF-D3NN is completely optimized based on frequency domain information because different objects have a very different Fourier transform pattern. Compared to networks based on spatial domain light intensity values, OF-D3NN statistically uses the different objects' intensity features of the different frequency distributions for training to accomplish complex tasks. Through training, the networks can reduce the impact of the three optical conditions listed above on the network performance. In addition, by injecting noise into the networks during the training process, we reduce the influence of the parameter errors caused by the network accuracy during the manufacturing process [14]. Finally, to demonstrate the performance of this network, we integrate it into FSO to improve the signal loss at the receiver.

## 2. THEORY

### A. Optical Forward Propagation

Previous work on D2NN was done to iteratively optimize the network parameters based on light intensity information through CCD or CMOS. In this process, the frequency information of the light is ignored. However, D2NN is proposed based on the Fourier optics theory. Fourier optics considers that the input optical signal is a weighted superposition of optical signals of different frequencies. Frequency information plays an important role in Fourier optics. Therefore, unlike traditional image processing techniques, we no longer set the input and output images as pure real numbers; instead, we pay more attention to the frequency distribution of the images [15,16].

When the signal  $U$  carries information, its amplitude and initial phase will change accordingly. For example, for plane light, its amplitude and phase at different positions are the same. According to the theory of angular spectrum diffraction, however, when it carries image information (any image can be seen as a superposition of a large number of sinusoidal gratings in different directions and different phases), the amplitude and phase at different positions of the secondary light source are no longer the same.  $U$  and  $U'$  are expressed as

$$U = \begin{bmatrix} a_0 & \cdots & a_0 \\ \vdots & \ddots & \vdots \\ a_0 & \cdots & a_0 \end{bmatrix} \cdot \begin{bmatrix} e^{i\varphi_0} & \cdots & e^{i\varphi_0} \\ \vdots & \ddots & \vdots \\ e^{i\varphi_0} & \cdots & e^{i\varphi_0} \end{bmatrix}, \quad (1)$$

$$U' = \begin{bmatrix} a_{11} & \cdots & a_{1n} \\ \vdots & \ddots & \vdots \\ a_{n1} & \cdots & a_{nn} \end{bmatrix} \cdot \begin{bmatrix} e^{i\varphi_{11}} & \cdots & e^{i\varphi_{n1}} \\ \vdots & \ddots & \vdots \\ e^{i\varphi_{1n}} & \cdots & e^{i\varphi_{nn}} \end{bmatrix}, \quad (2)$$

where  $a_0$  and  $\varphi_0$  are the amplitude and phase of  $U$ , respectively;  $a_{nn}$  and  $\varphi_{nn}$  are the amplitude and phase at different positions of  $U'$ , respectively; and  $n$  is the pixel value of  $U'$ .

In the frequency domain, light diffracted at a certain distance is equivalent to a certain shift in its phase without affecting its amplitude. Therefore, when the network only considers the spatial light intensity, it ignores a lot of information stored in the phase.

The network framework is shown in Fig. 1. Distortion occurs when the information is transmitted to the network due to the instability of the light source frequency or the channel. After the laser outputs coherent light, the target  $U_0$  is transformed into

the frequency domain through the lens to obtain  $U_i$ ,  $U_i = FU_0$ , where  $F$  is the Fourier transform matrix.  $U_i$  is the input to OF-D3NN to train the network and the network modulates the input light field  $U_i$  complexly, and the modulation function is  $W$ . By adding a photorefractive crystal, the light field propagates through a nonlinear material with a complex activation function  $\varphi$ , and the network's output light field is  $U_0$ ,  $U_0 = \varphi(WU_i) = \varphi(WFU_0)$ . Each artificial neuron has two modulation phases: phase and amplitude. For manufacturing convenience, only the phase modulation is used here, and the amplitude value is set to 1 [4]. The modulation function of each neuron is

$$t_i(x_i, y_i, z_i) = 1 \cdot \exp [j\phi_i^l(x_i, y_i, z_i)], \quad (3)$$

where  $\phi$  represents the modulation of the phase by the artificial neuron, and the range of  $\phi$  is restricted to  $0-2\pi$  using the sigmoid function for ease of fabrication. The OF-D3NN proposed in this paper does not need to perform an inverse Fourier transform to calculate the loss function by backpropagation after outputting  $U_0$ , but compares the difference between the two groups of complex numbers  $U_0$  and  $U_i$ .

### B. Loss Function

Compared to calculating the loss function in real space from the light intensity values of the input and output light fields, this method preserves more information and allows the networks to handle more complex tasks. After comparison, it is found that this approach can improve the network's modulation capability. The loss function is

$$F\_loss = \frac{1}{M} \sum_n \left( |\text{Real}_{gt} - \text{Real}_d| + |\text{Imag}_{gt} - \text{Imag}_d| \right), \quad (4)$$

where,  $\text{Real}_{gt}$ ,  $\text{Real}_d$  and  $\text{Imag}_{gt}$ ,  $\text{Imag}_d$  are the real and imaginary parts of the Fourier transform of the label and the input, respectively.  $n$  is the number of input samples per batch, and  $M$  is the number of pixels per sample. The resulting errors are backpropagated to iteratively update the phase modulation coefficients of the OF-D3NN and ultimately minimize the loss. After training, the OF-D3NN framework is fixed and the diffraction modulation coefficients are determined, to be ready for physical fabrication.

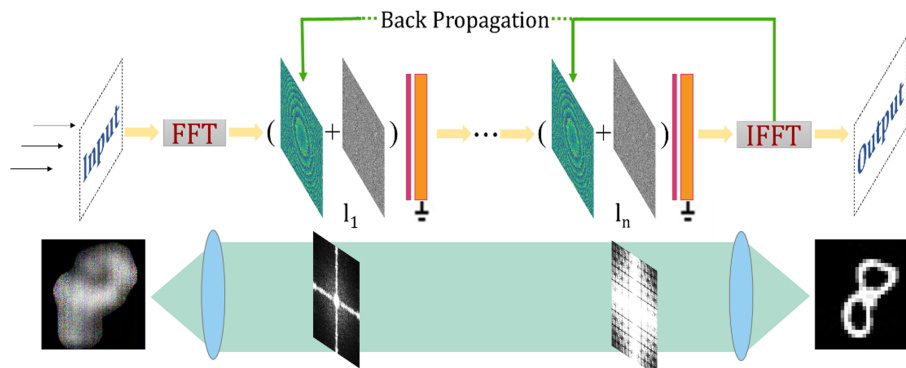


**Fig. 1.** Framework of OF-D3NN. OF-D3NN recovers such degraded signals due to light source or channel instability.

### C. Optical Nonlinearity Property

To improve the network's generalization ability, we use potassium sodium strontium barium niobite (KNSBN) as the activation function in this paper. As a photorefractive crystal with good nonlinearity and low absorption of light, KNSBN can achieve much a stronger optical nonlinear response than other optical nonlinear effects [12]. As a doped strontium barium niobate, KNSBN requires less laser power. The light intensity of KNSBN to turn on the photorefractive effect is low: only 0.13 mW/mm<sup>2</sup>. The corresponding time is related to the light intensity and incident angle of the input light, which is of the same order of magnitude as seconds. The change in the refractive index of a crystal can be modeled as

$$\Delta n = k E_{\text{app}} \langle I \rangle / (1 + \langle I \rangle), \quad (5)$$

where  $\langle I \rangle$  is the intensity perturbation above a spatially homogeneous background intensity,  $E_{\text{app}}$  is the applied electric field, and  $k$  is a constant depending on the properties of KNSBN.

### D. Optical Training Related Details

Consider that during manufacturing, whether using 3D printing or photolithography, the network's diffraction layer parameters will have errors due to problems with mechanical precision. Therefore, during the network training process, noise is randomly added to each network layer in each iteration [14]. This operation will cause the weight parameters of each network update to be biased due to noise injection, so that the network is trained to improve the network's robustness to errors caused by mechanical inaccuracies. Therefore, the update equation during the network training can be expressed as

$$\phi(s+1) = \phi(s) - \mu \frac{\partial \{y_t - \text{output}[x_t, \phi_n(s)]\}}{\partial \phi}, \quad (6)$$

where  $\phi(s)$  is a parameter that can be learned as the phase value of each neuron in the network,  $s$  is the number of iterations of the network parameters,  $\mu$  is the learning rate of the network,  $x_t$  and  $y_t$  are the input and label of the dataset, respectively, and  $\phi_n(s)$  is the phase value with added noise (that is,  $\phi_n(s) = \phi(s) + \text{noise}$ ). Because most noises approximately satisfy the Gaussian distribution, in this paper we choose to inject Gaussian noise; namely

$$\text{noise} \sim N(0, \sigma^2), \quad (7)$$

where  $\sigma$  is set as a network hyperparameter according to the actual environment to improve the network robustness without, as much as possible, losing the network's accuracy. Because noise is a common problem in deep learning networks, it is worth mentioning that network training with noise has been shown to widely improve network performance [17, 18]. Our research aims to enhance the robustness of optical diffraction networks to real-world errors; that is, to enable optical networks to maintain high-precision predictions in complex perturbed environments.

The data is passed through a Fourier lens before being input into the network, and the spatial domain information is converted into frequency domain information to train the network. The network modulates the information in the form of complex numbers, and the output of the network is still frequency

domain information. Then, the network is optimized by comparing the distribution differences of the input and output information of the network at different frequencies. At each iteration of the network parameters, the Gaussian error is injected into it until the network is trained. Finally, the network output is transformed back to the spatial domain through a Fourier lens for subsequent operations.

### 3. PERFORMANCE EVALUATION

We verify the effectiveness of the proposed network with two image processing tasks: image classification and imaging. All tasks were implemented using Python 3.6.0 and TensorFlow 1.4.0 as experimental platforms, using a Windows 10 system, Intel i7-8700 CPU at 3.2 GHz, 64.0 G RAM, and NVIDIA GeForce RTX 2080 Ti GPU. In this paper, each layer of the network consists of 200 × 200 neurons, each with a size of 1 μm. We test the classification effect of the network on the MNIST dataset [1] under the condition that the wavelength of the input light field is 980 nm. We compare the performance of two networks for image classification by using the same training method as the plain D2NN trained based on spatial light intensity in Ref. First, we randomly selected 2000 images from the MNIST dataset and upsample them to match the networks size. Then we randomly split these images into 1500 training images, 200 validation images, and 300 testing images. The final accuracy of the networks can reach 96.52% (plain D2NN is only 91.75%). Through the analysis of 500 images extracted from the dataset (50 images of each digit), it can be seen from Fig. 2 that OF-D2NN alleviates the problem of the reduced accuracy of plain D2NN for numbers with many blanks in spatial domain such as '0', '6,' and '9' [4]. In Table 1, we also compare the image recognition accuracy of plain D2NN, F-D2NN, and OF-D3NN when the transmitted information is distorted in varying degrees due to a frequency error caused by laser frequency noise or a Doppler shift. Note that OF-D3NN has stronger robustness to frequency errors. Due to similar loss functions, OF-D2NN and plain D2NN perform similarly.

For image restoration and image visualization, in Fig. 3 we demonstrate the imaging capabilities of the networks. Due to the frequency error caused by laser frequency noise or a Doppler frequency shift, plain D2NN will further degrade the image quality, while OF-D3NN can restore the image quality. We quantitatively analyze the influence of different networks on the image quality in Table 2. Compared to plain D2NN, OF-D3NN improves the peak SNR (PSNR) and structural similarity index measure (SSIM) by 61.40% and 315.98% for image restoration, respectively.

The two typical image processing tasks above, show that OF-D3NN has an excellent ability to suppress frequency noise compared to plain D2NN. Since plain D2NN is only designed for a specific single frequency, when the frequency of the light source or channel is disturbed, it is difficult for plain D2NN to play a role and even further disturbs the information. The special design of OF-D3NN enables the diffraction networks to find regions that are not sensitive to frequency changes, thereby improving the networks' robustness to frequency.

We also tried to integrate OF-D3NN into FSO. As a key technology to solve the last mile problem of broadband networks

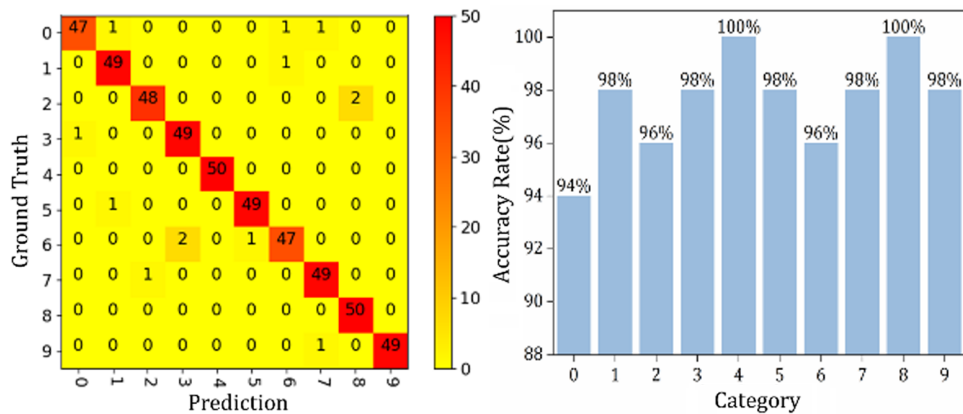


**Fig. 2.** Confusion matrix and accuracy per group of digits. OF-D3NN recognizes different digits with similar accuracy.

**Table 1. Comparison of Image Reconstruction Accuracy Under Different Levels of Noise**

<b>PSNR</b>	<b>100.00</b>	<b>31.73</b>	<b>21.29</b>	<b>16.41</b>
Plain D2NN	91.75%	83.41%	71.40%	61.52%
F-D2NN	94.66%	83.98%	75.06%	63.79%
OF-D3NN	96.52%	93.48%	89.03%	86.31%

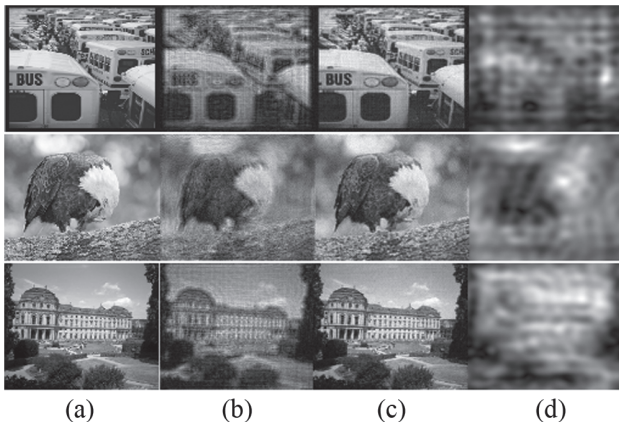


**Fig. 3.** Comparison of image restoration quality on different networks: (a) original image; (b) image with frequency error; (c) image generated by OF-D3NN; and (d) network generated by plain D2NN.

**Table 2. Image Quality Comparison**

	<b>Original Image</b>	<b>Noisy Image</b>	<b>Plain D2NN</b>	<b>F-D2NN</b>	<b>OF-D3NN</b>
PSNR	100.00	16.98	13.03	13.37	21.03
SSIM	1.0	0.4655	0.2021	0.2283	0.8407

communications, FSO is valued by academia and industry [19]. Since most FSOs use semiconductor lasers to transmit signals, they are still affected by frequency noise. This noise mainly comes from the intrinsic noise of a laser's spontaneous emission, external interference noise caused by external vibration and temperature drift, and atmospheric turbulence [20,21]. We verified the performance of OF-D3NN for signal recovery in an FSO by testing the ability of OF-D3NN to compress the laser

linewidth and recover the signal wavefront distortion caused by atmospheric turbulence.

Due to the inherent linewidth problem, the laser's output light field can be expressed as

$$E(t) = E_0 \exp[j(-\omega_0 t + \varphi(t))], \quad (8)$$

where  $E_0$  and  $\omega_0$  are the stable amplitude and frequency of the laser, and  $\varphi(t)$  is the phase fluctuation of the laser. According to the Wiener–Khinchin theorem, its power spectral density is expressed as

$$S_E(f_x, f_y) = \int_{-\infty}^{+\infty} \langle E(t) E^*(t - \tau) \rangle e^{-j2\pi f \tau} dt, \quad (9)$$

where  $\tau$  is the random fluctuation time of the phase, and  $f$  is the frequency after Fourier transform. Due to random fluctuations in the air temperature during transport, the atmosphere exhibits a state of rough turbulence. These turbulences cause the atmospheric refractive index to vary randomly in space and time, resulting in different phase changes in the beam at different locations [20]. Atmospheric turbulence will cause a phase distortion of the received signal, the most common is the Kolmogorov turbulence model, whose power spectral density is

$$\varphi_n(K, Z) = 0.033 C_n^2(z) K^{-11/3}, \quad (10)$$

where  $Z$  is the beam propagation direction,  $C_n^2(z)$  is the structural constant of the turbulence intensity in the beam propagation direction, and  $K$  is the 3D spatial wavenumber. The atmospheric phase power spectrum perpendicular to the propagation direction ( $Z$  axis direction) is

$$F_\varphi(K_r) = 2\pi k^2 0.033 K_r^{-11/3} \int_z^{z+\Delta z} C_n^2(\xi) d\xi, \quad (11)$$

where  $\Delta z$  is the thickness of the turbulent flow,  $K_r = \sqrt{K_x^2 + K_y^2}$ , and  $K_z = 0$ . Since the linewidth of common semiconductor lasers is mainly concentrated in the range of 20–300 kHz, in the experiment, we set the linewidth of the laser to 300 kHz to test the network linewidth compression. As shown in Fig. 4, by comparing the frequency distribution of the network input and output signals, the laser phase noise suppression effect is obvious after the signal is modulated by the

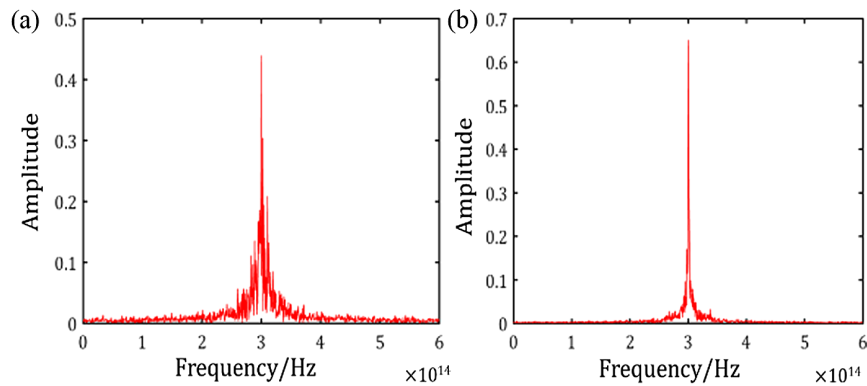


**Fig. 4.** Laser frequency distribution: (a) input signal distribution and (b) output signal distribution.

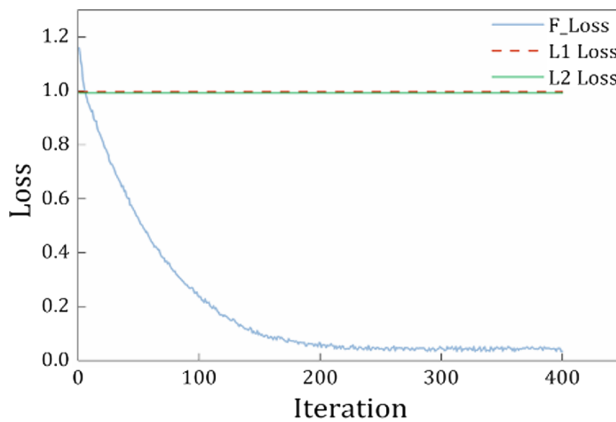


**Fig. 5.** Training loss of the diffraction networks based on different loss functions within 400 iterations.

networks, and the network output laser linewidth is reduced to 19.2 kHz.

At the same time, Fig. 5 shows that, compared to OF-D3NN, the diffraction network optimized by L1 loss and L2 loss functions that depend on the spatial intensity difference cannot learn the characteristics of the laser linewidth. During training, L1 loss and L2 loss is maintained at 0.996 and 0.992, respectively. OF-D3NN, which is more in line with the propagation of light, can retain more information.

On the basis of the laser frequency noise, we further process the image to recover its phase distortion due to atmospheric turbulence. Figure 6 shows the wavefront phase distribution of the image before and after restoration. The rms of the phase fluctuation before restoration is 3.5422 rad, and the rms of the phase fluctuation after restoration is 0.6385 rad.

The column diagram of the image's frequency is used for further analysis [21]. The column graph compares the distribution characteristics of the simulated image and the image intensity before and after restoration by counting the number of pixels occupied by each intensity of the image. Figure 7 shows that the strength distribution of the image after recovery is similar to the simulation image, and the consistency reaches 84.33%. Note that the consistency of the previous image and the simulation image strength is 20.82%.

In addition, we also analyzed the robustness of the networks to turbulent intensity, signal transmission distance, and laser

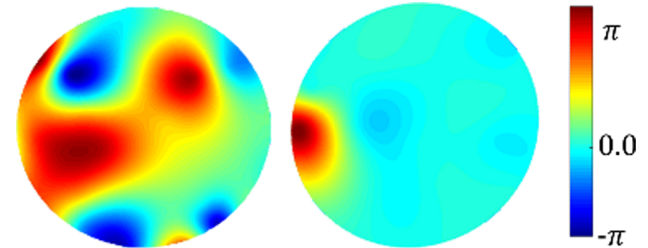


**Fig. 6.** Waves of front phase correction results: (left) random static wavefront and (right) corrected wavefront. Recovered wavefront phase fluctuations are reduced.

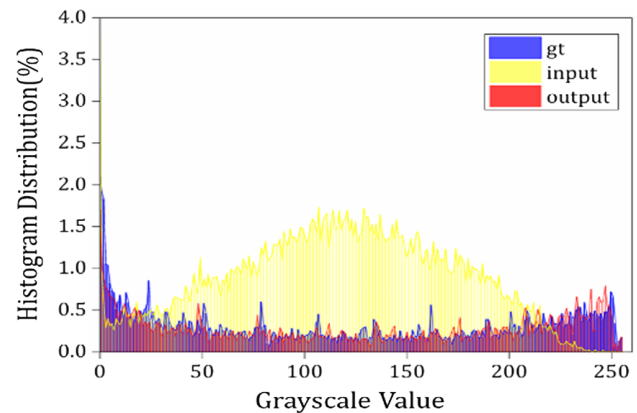


**Fig. 7.** Image strength folding line diagram. gt, input and output are the original image, the input and output images of the network, respectively.

linewidth. We changed the turbulence intensity  $C_n^2(m^{-2/3})$  and the transmission distance  $d$  to test the network performance, and used the two indicators (PSNR and SSIM) for quantitative analysis. As shown in Fig. 8, when the transmission distance  $d$  is certain, as the turbulence strength  $C_n^2$  increases, the image clarity decreases. When the turbulent intensity  $C_n^2$  is certain, the image gradually blurred with an increase in the transmission distance  $d$ .

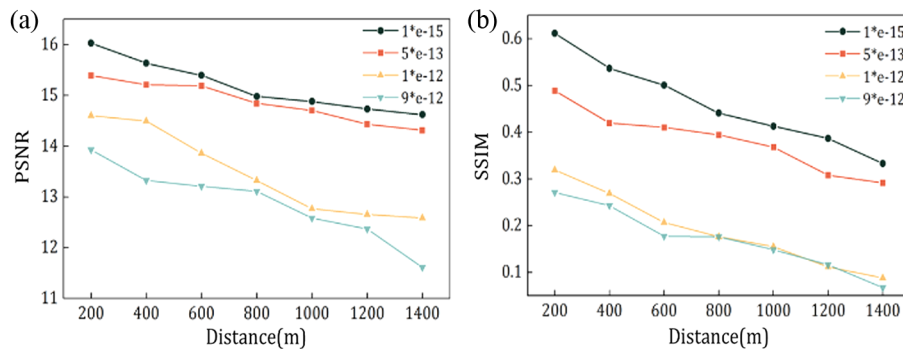


**Fig. 8.** Different turbulence intensity and image quality values at the transmission distance.

#### 4. CONCLUSION

In short, we have proposed a diffraction network structure that fully uses frequency information, and proved that it can show higher robustness compared to plain diffraction network processing image tasks. Using a laser as an information transmission carrier has higher practical significance for the network structure. In addition, we successfully integrated OF-D3NN into an FSO, which will help the system handle complex and realistic environmental denoising and information recovery.

**Funding.** National Natural Science Foundation of China (52171343); Dalian High Level Talents Innovation Support Plan (2019RJ08); Dalian Key Field Innovation Team (2021RT05); Liaoning Province “Unveiling the List and Taking the Lead” Project (85210038); Fundamental Research Funds for the Central Universities (3132021230).

**Disclosures.** The authors declare no conflicts of interest.

**Data availability.** No data were generated or analyzed in the presented research.

#### REFERENCES

- Y. L. Cun, Y. Bengio, and G. Hinton, “Deep learning,” *Nature* **521**, 436–444 (2015).
- Y. Deng, F. Bao, Y. Y. Kong, Z. Q. Ren, and Q. H. Dai, “Deep direct reinforcement learning for financial signal representation and trading,” *IEEE Trans. Neural Netw. Learn. Syst.* **28**, 653–664 (2017).
- J. M. Shainline, S. M. Buckley, R. P. Mirin, and S. W. Nam, “Superconducting optoelectronic circuits for neuromorphic computing,” *Phys. Rev. Appl.* **7**, 034013 (2017).
- X. Lin, Y. Rivenson, N. T. Yardimci, M. Veli, Y. Luo, M. Jarrahi, and A. Ozcan, “All-optical machine learning using diffractive deep neural networks,” *Science* **361**, 1004–1008 (2018).
- T. K. Zhou, X. Lin, J. M. Wu, Y. T. Chen, H. Xie, Y. P. Li, J. T. Fan, H. Q. Wu, L. Fang, and Q. H. Dai, “Large-scale neuromorphic optoelectronic computing with a reconfigurable diffractive processing unit,” *Nat. Photonics* **15**, 367–373 (2021).
- J. Feldmann, N. Youngblood, C. D. Wright, H. Bhaskaran, and W. H. P. Pernice, “All-optical spiking neurosynaptic networks with self-learning capabilities,” *Nature* **569**, 208–214 (2019).
- M. Veil, D. Mengu, N. Yardimci, L. Yi, L. Jingxi, R. Yair, J. Mona, and A. Ozcan, “Terahertz pulse shaping using diffractive surfaces,” *Nat. Commun.* **12**, 37 (2021).
- A. Silva, F. Monticone, G. Castaldi, V. Galdi, A. Alù, and N. Engheta, “Performing mathematical operations with metamaterials,” *Science* **343**, 160–163 (2014).
- C. Guo, M. Xiao, M. Minkov, Y. Shi, and S. H. Fan, “Photonic crystal slab Laplace operator for image differentiation,” *Optica* **5**, 251–256 (2018).
- N. M. Estakhri, B. Edwards, and N. Engheta, “Inverse-designed metastructures that solve equations,” *Science* **363**, 1333–1338 (2019).
- C. Qian, X. Lin, X. Lin, J. Xu, Y. Sun, E. Li, B. Zhang, and H. Chen, “Performing optical logic operations by a diffractive neural network,” *Light Sci. Appl.* **9**, 59 (2020).
- T. Yan, J. Wu, T. Zhou, H. Xie, F. Xu, J. Fan, L. Fang, X. Lin, and Q. Dai, “Fourier-space diffractive deep neural network,” *Phys. Rev. Lett.* **123**, 023901 (2019).
- J. Shi, Y. Chen, and X. Zhang, “Broad-spectrum diffractive network via ensemble learning,” *Opt. Lett.* **47**, 605–608 (2022).
- J. Shi, M. Chen, D. Wei, C. Hu, J. Luo, H. Wang, X. Zhang, and C. Xie, “Anti-noise diffractive neural network for constructing an intelligent imaging detector array,” *Opt Express* **28**, 37686–37699 (2020).
- C. Du, C. Du, L. Huang, H. Wang, and H. He, “Structured neural decoding with multitask transfer learning of deep neural network representations,” *IEEE Trans. Neural Netw. Learn. Syst.* **33**, 600–614 (2022).
- W. Neng, J. Lu, and L. Xu, “CCRRSleepNet: a hybrid relational inductive biases network for automatic sleep stage classification on raw single-channel EEG,” *Brain Sci.* **11**, 456 (2021).
- C. M. Bishop, “Training with noise is equivalent to Tikhonov regularization,” *Neural Comput.* **7**, 108–116 (1995).
- Y. Luo, D. Mengu, N. T. Yardimci, Y. Rivenson, M. Veli, M. Jarrahi, and A. Ozcan, “Design of task-specific optical systems using broadband diffractive neural networks,” *Light Sci. Appl.* **8**, 112 (2019).
- Z. Wang, W. D. Zhong, S. Fu, and C. Lin, “Performance comparison of different modulation formats over free-space optical (FSO) turbulence links with space diversity reception technique,” *IEEE Photon. J.* **1**, 277–285 (2009).
- K. Wang, M. Zhang, J. Tang, L. Wang, L. Hu, X. Wu, W. Li, J. Di, G. Liu, and J. Zhao, “Deep learning wavefront sensing and aberration correction in atmospheric turbulence,” *PhotonX* **2**, 8 (2021).
- L. Zhang, Z. Bian, H. Ye, Z. Wang, K. Wang, and D. Zhang, “Restoration of single pixel imaging in atmospheric turbulence by Fourier filter and CGAN,” *Appl. Phys. B* **127**, 45 (2021).